

CHROM. 21 038

## THE SEPARATION PROCESS IN ISOTACHOPHORESIS

### I. A 32-CHANNEL ULTRAVIOLET-PHOTOMETRIC ZONE DETECTOR

TAKESHI HIROKAWA\*, KIYOSHI NAKAHARA and YOSHIYUKI KISO

*Applied Physics and Chemistry, Faculty of Engineering, Hiroshima University, Shitami, Saijo, Higashi-hiroshima 724 (Japan)*

(First received March 23rd, 1988; revised manuscript received September 12th, 1988)

---

#### SUMMARY

Multichannel ultraviolet (UV)-photometric zone detector was made in order to study the separation process in isotachopheresis. Thirty-two photometric cells with photodiode detectors were arrayed along the separation tube at intervals of *ca.* 5 mm (16.6 cm per 32 channels). Quartz optical fibres were used to pass UV light from a deuterium lamp to the tube. The detection limit of picric acid was *ca.* 10 pmol. The time resolution achieved in this system, a single cycle to scan the 32 detectors, was *ca.* 0.25 s by the use of an electrical scanning method, and it was sufficiently high to trace the variation of the zone lengths accurately. Using the apparatus, the separation process in binary mixtures [4,5-dihydroxy-3-(*p*-sulphophenylazo)-2,7-naphthalene-disulphonic acid and monochloroacetic acid, and monochloroacetic acid and picric acid] was measured and the boundary velocities and the resolution time were evaluated.

---

#### INTRODUCTION

A computer simulation of the isotachopheretic steady state<sup>1</sup> can be applied to the estimation of the optimum separation condition<sup>2</sup>. We have demonstrated the utility of this technique in practical analysis of many ionic substances. Simulated quantitative and qualitative indices have been tabulated for 287 anions<sup>3</sup>. However, the information obtained by steady state simulation is limited to the static properties of the separated zones<sup>3,4</sup>. In order to study the dynamics of separation, the simulation of the isotachopheretic transient state is inevitable. The resulting resolution time of the samples provides the criterion for the separation under the electrolyte and apparatus conditions used.

The resolution time for samples in isotachopheresis is closely related to the velocities of the mixed zone boundaries as extensively discussed by Mikkers *et al.*<sup>5,6</sup>. However the velocities have not been measured yet even for binary mixtures and all discussions concerning the dynamic features of isotachopheresis were based on the resulting resolution time. Moreover the fundamental problem of whether the progression of the mixed zone boundaries can be described by linear functions of time has not been solved.

As detailed in the following paper, some different transient state models can be formulated. To obtain knowledge concerning the validity of these models, a zone scanning analyzer is indispensable to observe both the resolution time and the boundary velocity and to compare them with the theoretical estimates. For this purpose the time resolution of the analyzer must be sufficiently high for accurate observation of the separation process. Schumacher<sup>7,8</sup> reported a multichannel isotachophoretic analyzer equipped with an equidistant array of 256 detection electrodes (total length = *ca.* 10 cm) for observation of the potential gradient profile of the transient zones. Although Thormann *et al.*<sup>8,9</sup> studied the separation process of some organic acids using this system, the resolution time and boundary velocities were not reported.

In the apparatus reported<sup>7,8</sup>, complex electronic circuits were necessary to isolate potential gradient detector signals from high voltage. Considering the convenience of construction, we designed a 32-channel UV photometric detection system. And an electrical scanning method was used to improve the time resolution instead of a mechanical scanning method<sup>7,8</sup>.

In this paper we report the design and the detection limit of the UV detection system. The abilities to observe the resolution time and the velocity of the zone boundaries are also discussed for binary mixtures.

## EXPERIMENTAL

### Apparatus

Fig. 1 shows a schematic diagram of the UV-multichannel detection system. The length of the UV-photocell arrays to be scanned was 16.6 cm and the interval of

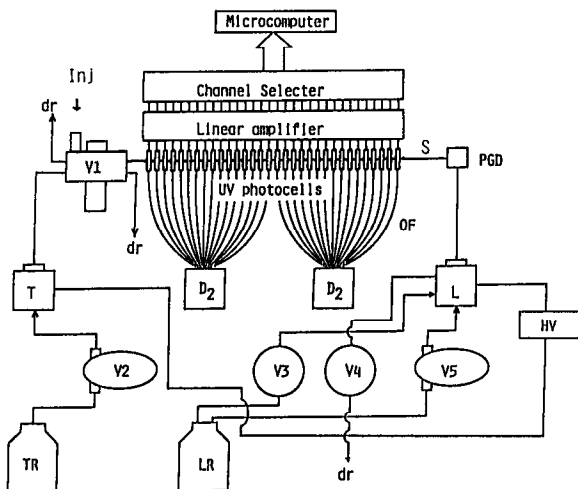


Fig. 1. Schematic diagram of isotachophoretic analyzer with 32-channel UV-photometric zone detector. S = PTFE separating tube; D<sub>2</sub> = D<sub>2</sub> lamp with power supply; OF = quartz optical fibres; L = leading electrode compartment; T = terminating electrode compartment; Inj = injection port; LR and TR = leading and terminating electrolyte reservoirs; V1-V5 = valves to fill or to drain the electrolytes; dr = drain; PGD = potential gradient detector; HV = high voltage power supply.

photocells was *ca.* 5 mm. The length of the photocell array was determined such that the transient state could be observed during 40 min under conditions where the leading ion was 5 mM Cl<sup>-</sup> and the migration current was 50  $\mu$ A.

A narrow-bore migrating tube penetrated the centre of 32 photocells, which were made of black acrylic resin (20  $\times$  20  $\times$  3 mm). The separating tube was made of PTFE and the I.D. and O.D. were 0.5 mm and 1 mm. The tube was irradiated by UV light from quartz optical fibres (OF in Fig. 1). The core and clad diameters were 0.8 mm and 1.1 mm, respectively. The fibres were set at right angles to the separating tube. The transmitted UV light was led to short-cut optical fibres (*ca.* 10 mm in length) plugged into the cell. Therefore the slit width of each photocell can be regarded as *ca.* 1 mm. At the end of the fibres were placed detection elements. The elements used were Model S1227-16BQ silicone photodiodes (15  $\times$  2.7  $\times$  2 mm) Hamamatsu, Japan. Each photodiode was equipped with a head amplifier using LF356N and LM741CN operational amplifiers.

The UV-light source was two Hamamatsu D<sub>2</sub> lamps (Model L1626, D<sub>2</sub> in Fig. 1) set separately in a box equipped with a cooling fan. The lamps were driven by an independent power supply (Hamamatsu Model C1518). The UV light from each D<sub>2</sub> lamp was led to 16 optical fibres through an UV-glass filter (Toshiba Glass, Tokyo, Japan, Model D33S,  $\lambda_{\max}$  = 330 nm).

To obtain high time resolution, an electrical channel selector using analogue switches was utilized for scanning the UV signals from the head amplifiers. This was in contrast to the mechanical scanning of the electrodes in the multichannel detection system reported by Schumacher *et al.*<sup>7,8</sup>. By the control of a microcomputer system through an RS-232C line, the selector scanned the 32 detectors and the signal detected at each channel were successively acquired through an analogue-to-digital converter and subsequently stored in the 2MB random access memory (a RAM disk system) of the microcomputer. The use of the RAM disk system is important for rapid data acquisition. A single cycle to scan the 32 detectors per 16 cm, namely the time resolution of the system, was 243.2 ms. The rate-determining step was the transfer of the channel selection signal through the RS-232C line (9600 Baud). The time resolution was considerably improved in comparison with the previous multichannel analyzer<sup>7,8</sup> where it took *ca.* 30 s to scan the 255 detectors per 10 cm (data acquisition, 60 ms  $\cdot$  255; moving back to the first channel, 14 s).

Usually the number of data acquired was 5000–7000 per channel. After the acquisition was completed, the data in the RAM disk were transferred to a floppy disk. The data were evolved and analyzed to obtain the boundary velocities as discussed in a subsequent section. Since the levels of the acquired signals from each detector were different, they were normalized appropriately by multiplying factors.

Except for the detection system, the parts used were those of a commercial isotachophoretic analyzer (Model IP-1B, Shimadzu, Kyoto, Japan). The power supply was from a Shimadzu IP-2A. The distance from the injection port to the first photocell was about 16 cm. A potential gradient detector (PGD in Fig. 1) was placed at the end of the migrating tube, 5 cm from the 32nd photocell.

### Samples

The samples were 4,5-dihydroxy-3-(*p*-sulphophenylazo)-2,7-naphthalene disulphonic acid (SPADNS), picric acid (PIC) and monochloroacetic acid (MCA). Except

for MCA, these samples absorb visible and ultraviolet light. The sodium salt of SPADNS was obtained from Dojin (Kitakyusyu, Japan) in the most pure form. The others were obtained from Tokyo Kasei (extra pure grade). Stock sample solutions (ca. 10 mM) were prepared by dissolving them in distilled water without further purification.

#### *Operational electrolyte system*

The concentration of the sample to be separated is closely related with that of the leading ion. For the SPADNS and MCA (1:1) system, the leading electrolyte was 10 mM hydrochloric acid. The pH was adjusted to 3.6 by adding  $\beta$ -alanine. For the MCA and PIC (1:1) system, the difference between the UV absorption of the mixed zone and that of the PIC zone was small when the 10 mM leading electrolyte was used, therefore in this case a 5 mM leading electrolyte was used for accurate boundary observation. The 2.5 mM leading electrolyte was used only for the sensitivity evaluation of PIC. The pH measurements were carried using a Model F7ss expanded pH meter (Horiba, Tokyo, Japan).

The terminator was 10 mM caproic acid. The sample solution was injected into the terminating electrolyte near the boundary between the leading and the terminating electrolytes.

Hydroxypropylcellulose (HPC, 0.2%) (Tokyo Kasei, Tokyo, Japan) was added to the leading and terminating electrolytes to suppress electroendosmosis. The viscosity of the 2% aqueous solution is 1000–4000 cP at 20°C according to the specification. The reproducibility of the observed boundary velocity was not so good when the HPC concentration was low, e.g., 0.02%. The other cause of this was temperature variation. Although the apparatus was set in a thermostatted room (25°C), the experimental errors of a few percent could not be reduced.

The data processing was carried by the use of Model PC9801E and PC9801VX microcomputers (NEC, Tokyo, Japan). A Model DXY-980 (Roland DG, Tokyo, Japan) was used to plot the evolved pherograms.

## RESULTS AND DISCUSSION

### *Sensitivity evaluation*

Isotachopherograms of picric acid were obtained to estimate the practical detection limit of the system used by varying the injected amount in the range of 16 pmol–5 nmol (injected volume 1–5  $\mu$ l). The concentration of the leading ion was 2.5 mM. Fig. 2 shows the observed UV response at 1–31 channels (interval: two channel) together with the blank test. The abscissa scale is the time of migration and the ordinate scale is the observed UV absorption. The position of baselines shows the distance of each UV photocell from the sample injection port. Apparently, 16 pmol picric acid were detected.

Arlinger<sup>10</sup> discussed the resolution and detection limits of isotachopheresis using an UV detector. The capillary diameter was 0.45 mm and the slit width of the detector was chosen as 0.2 mm. When a leading electrolyte of 0.5 mM hydrochloric acid–1 mM histidine was used (pH 5.98, 0.01% Triton X-100), the detection limit of adenosine triphosphate ion was 1 pmol. This result is comparable with that of the present work considering the difference in the leading ion concentrations.

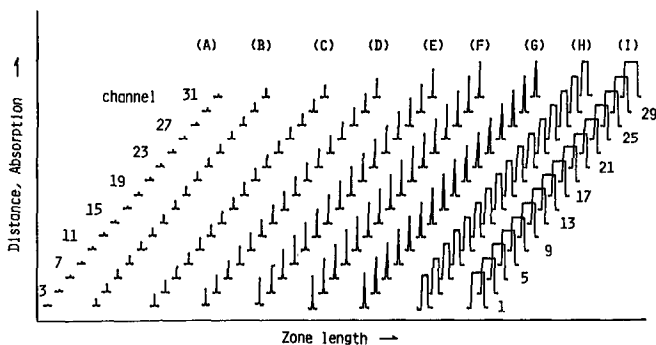


Fig. 2. Detection limit of picric acid by the use of the 32-channel UV-photometric detector. The position of the baselines shows the distance of the photocell from the sample injection port. (A) Blank test; (B) 15.7, (C) 39.2, (D) 62.7, (E) 157, (F) 313, (G) 627, (H) 2507 and (I) 5013 pmol. The leading ion was 2.5 mM hydrochloric acid (pH 3.6, buffer =  $\beta$ -alanine). The terminator was 10 mM caproic acid. The migration current was 24.5  $\mu$ A. The I.D. of the separation tube was 0.54 mm.

Quantitative analysis in isotachopheresis using an UV detector can be achieved by analyzing the width of the zones in the case when the zone length is sufficiently larger than the slit width, e.g., 5 nmol, (I) in Fig. 2. However, when the zone length is similar to or smaller than the width, the UV absorption band observed will have a quasi-Gaussian shape. As discussed by Svoboda and Vacík<sup>11</sup>, in such a case the peak height is useful for determination; a linear relationship holds between the relative photometric height and the amount of sample injected.

The peak area can be utilized similarly instead of the peak height. Fig. 3 shows the relationship between the observed peak area in arbitrary units and the amount of picric acid. The gradient of the plots over ca. 1 nmol was different from that below ca. 1 nmol. According to our simulation, the zone length of 1 nmol picric acid is 3.2 mm under the electrolyte condition used. The length was three times as large as the clad diameter of the optical fibres used.

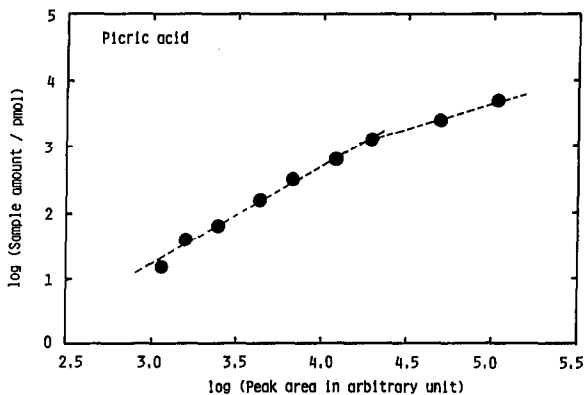


Fig. 3. The UV peak area in arbitrary units vs. sample amount of picric acid. The sample amount was varied from 15.7 to 5013 pmol. For the operational system, see Fig. 2.

The detection limit of picric acid is probably *ca.* 10 pmol. By the use of digital data processing, and if necessary appropriate UV-transparent spacers, the detection limit in isotachopheresis is probably comparable with those of high-performance liquid chromatography (HPLC) and capillary zone electrophoresis.

#### *Separation process of the binary mixtures*

Under the electrolyte condition used, the samples were detected in the order of SPADNS, MCA and PIC. To measure the separation process as ideally as possible, it is preferable to sandwich the sample solution by the leading and the terminating electrolytes at the initial stage. However, in this work the sample was injected into the terminating electrolyte near the interface of the leading and terminating electrolytes by use of a micro-syringe. Although the partial mixing of the sample solution and the terminating electrolyte was indispensable, no mixed zone between the sample and the terminator was observed. When the sample solution was injected into the leading electrolyte, however, the formation of a mixed zone of the leading ion and the most mobile sample ion was frequently observed.

Fig. 4 shows the evolution of a transient isotachopherogram of SPADNS and MCA, where the mixed zone of the leading ion and SPADNS was seen. The number of data used for the evolution was 3500 per channel. Before starting migration, in this particular case, the injected sample zone was forced to move toward the terminating electrolyte compartment. In Fig. 4, the boundaries between the terminating and the

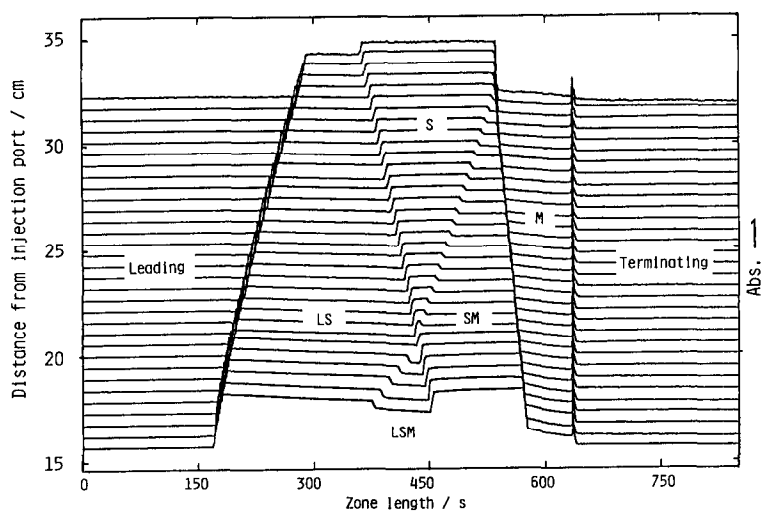


Fig. 4. Transient isotachopherogram of SPADNS and monochloroacetic acid observed by the use of the 32-channel UV-photometric detector. The injected sample zone was pushed toward the terminating electrolyte compartment. The position of baselines of the UV absorption shows the distance of the photocell from the sample injection port. The observed boundaries between the terminating and the preceding MCA zones were rearranged at the same abscissa position. Samples: 5 mM SPADNS(S); 5 mM monochloroacetic acid (M), 10  $\mu$ l. LS, LSM and SM denote the mixed zones formed among the leading ions(L), SPADNS(S) and monochloroacetate ions(M). The leading electrolyte was 1 mM hydrochloric acid and the pH was adjusted to 3.6 (buffer  $\beta$ -alanine). The terminating electrolyte was 10 mM caproic acid. The migration current was 98.4  $\mu$ A. The I.D. of the separation tube was 0.51 mm.

preceding MCA zones were rearranged at the same abscissa position to demonstrate clearly the change in the individual zone length at the transient state. This procedure corresponds to the situation of 100% counterflow of the solvent. Considering the fact that the UV absorption was due to SPADNS and the concentrations in each zone were different from each other and all of the width-decreasing zones were mixed zones, the different zone found in Fig. 4 can easily be assigned as shown. Besides the mixed zone of the leading ion ( $\text{Cl}^-$ ) and SPADNS(LS) and that of SPADNS and MCA(SM), a mixed zone of all of them (LSM) was seen. However that of the terminating ion (caproate) and MCA not observed.

Fig. 5 shows the transient isotachopherograms of a 1:1 mixture of SPADNS and MCA obtained under the usual conditions. The number of data used for the evolution was 1200 per channel. The boundaries between the terminating and the preceding PIC zones were rearranged at the same abscissa position. A small amount of PIC was added to the mixture to distinguish the terminating zone. The sample concentration was 1.25 mM. The sample amounts were (A) 40, (B) 50 and (C) 60 nmol. The mixed zone observed was due to SPADNS and MCA. The small peak adjacent to the terminating zone was due to the absorption of PIC. The zone imposed by the peak and the mixed zone (SM), the width of which was increasing, is that of MCA(M). It is apparent from Fig. 5A that the progression of the boundaries can be expressed by linear functions with respect to time. The boundary velocity of S/SM was smaller than the isotachopheretic velocity,  $V_{IP}$ , and that of SM/M was larger than  $V_{IP}$ . The time-based zone lengths of the whole sample zones were almost constant during detection. After the mixed zones were diminished, the zone lengths of the separated samples were constant.

In order to determine the boundary-detected time and subsequently the boundary velocity, the observed UV signals were differentiated with respect to time and the positive and negative peaks of the differentiated signals were searched. Table

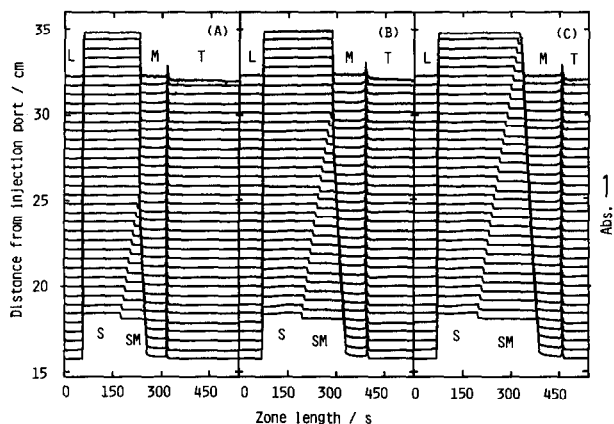


Fig. 5. Transient isotachopherogram of SPADNS(S) and monochloroacetic acid(M) observed by the use of the 32-channel UV-photometric detector. The sample concentration was 1.25 mM and the amounts were (A) 40, (B) 50 and (C) 60 nmol. SM = Mixed zone; L, T = the leading and terminating zones. For the operational system, see Fig. 4.

TABLE I

THE DETECTOR POSITION, BOUNDARY-DETECTED TIME AND TIME-BASED ZONE LENGTH FOR THE SPADNS AND MONOCHLOROACETIC ACID (1:1) SYSTEM

Operational system: leading electrolyte, 10 mM hydrochloric acid- $\beta$ -alanine (pH 3.60). Current: 98.4  $\mu$ A. Diameter of the separation tube: 0.51 mm. Sample concentration: 1.25 mM. Sample amounts: each 40 nmol. —, Did not exist; ?, the exact boundary positions could not be estimated.

Detector position		Boundary-detected time (s)					Overall zone length (s)
No.	mm	L/S	S/SM	S/M	SM/M	M/T	
1	0	470.8	586.4	—	665.2	726.7	256.0
2	5.4	486.8	606.5	—	679.5	741.8	255.0
3	10.5	502.4	626.5	—	693.6	758.4	256.0
4	15.9	519.0	647.7	—	709.0	774.7	255.7
5	21.2	535.0	667.9	—	723.6	791.0	256.0
6	26.5	551.8	689.0	—	738.6	808.0	256.2
7	31.8	567.9	708.7	—	753.5	823.6	255.7
8	37.1	584.2	730.0	—	768.3	840.4	256.2
9	42.4	600.2	750.3	—	783.2	856.2	256.0
10	47.4	615.8	769.3	—	797.3	872.2	256.4
11	53.0	632.8	791.2	—	812.6	889.0	256.2
12	58.5	649.9	812.1	—	827.9	905.3	255.5
13	63.9	665.9	833.3	—	843.0	922.1	256.2
14	69.1	682.5	853.7	—	857.8	938.9	256.4
15	74.6	699.2	?	?	?	955.2	256.0
16	79.9	716.0	(173.7)*	889.7	(81.8)**	971.5	255.5
17	85.3	732.8	(173.7)	906.5	(81.5)	988.0	255.2
18	90.8	749.6	(173.7)	923.3	(81.0)	1004.3	254.7
19	96.1	766.4	(173.7)	940.1	(81.3)	1021.4	255.0
20	101.4	782.7	(173.5)	956.2	(81.8)	1038.0	255.2
21	106.9	799.5	(173.5)	973.0	(81.8)	1054.7	255.2
22	112.3	816.0	(173.7)	989.7	(82.0)	1071.7	255.7
23	117.8	832.8	(173.7)	1006.5	(81.8)	1088.3	255.5
24	123.1	848.9	(174.0)	1022.8	(81.8)	1104.6	255.7
25	128.4	865.7	(173.7)	1039.4	(81.8)	1121.1	255.5
26	133.6	881.7	(173.7)	1055.5	(82.0)	1137.4	255.7
27	138.9	898.0	(173.7)	1071.7	(81.8)	1153.5	255.5
28	144.2	914.6	(173.7)	1088.3	(81.5)	1170.0	255.2
29	149.6	930.6	(173.7)	1104.3	(81.8)	1186.1	255.5
30	154.8	947.2	(173.5)	1120.6	(82.0)	1202.6	255.5
31	160.2	963.5	(173.7)	1137.2	(81.8)	1218.9	255.5
32	165.5	979.5	(174.0)	1153.5	(82.0)	1235.5	256.0

\* Zone length(s) of SPADNS.

\*\* Zone length(s) of MCA.

I summarizes the boundary-detected time at each detector after starting the separation of SPADNS and MCA for the 40-nmol case. The boundary velocities can be evaluated by the least-squares method on the basis of these numerical data.

The resolution time,  $t_{res}$ , of a binary mixture (components A and B, effective mobility of A larger than that of B) can be expressed as follows<sup>5</sup>

$$t_{res} = l_A / (V_{IP} - V_{A/AB}) \quad (1)$$



TABLE II

## OBSERVED BOUNDARY FUNCTIONS FOR THE SPADNS-MONOCHLOROACETIC ACID (1:1) SYSTEM AND THE RESOLUTION TIME

For the operational system, see Table I.  $V$  = Boundary velocity ( $\text{mm s}^{-1}$ )  $\cdot 10$ .  $D$  = The observed intercepts of the boundary functions; the first detector position is the frame of reference.  $D_0$  = The intercepts; the initial position of the leading electrolyte observed is the frame of reference.  $t_{\text{res}}$  = Resolution time.

	Sample amount (nmol)								
	40			50			60		
	$V$	$D$	$D_0$	$V$	$D$	$D_0$	$V$	$D$	$D_0$
L/S	3.246	-152.5	0	3.250	-158.6	0	3.224	-157.3	0
S/SM	2.583	-151.4	1.1	2.607	-158.1	0.5	2.582	-157.3	0
S/M	3.246	-209.0	-56.5	3.297	-232.8	-74.2	-	-	-
SM/M	3.579	-237.9	-85.4	3.616	-267.5	-108.9	3.579	-284.7	-127.4
M/T	3.249	-235.8	-83.3	3.287	-264.8	-106.2	3.238	-280.8	-122.2
$t_{\text{res}}(\text{s})$	868			1007			1222		

where  $l_A$  is the zone length of the component A at the steady state,  $V_{\text{IP}}$  the isotachophoretic velocity and  $V_{\text{A/AB}}$  the boundary velocity of A/AB. Eqn. 1 can be rewritten in terms of the time-based zone length of component A,  $t_A$

$$t_{\text{res}} = t_A / (1 - V_{\text{R,A/AB}}) \quad (2)$$

where  $V_{\text{R,A/AB}}$  is the velocity ratio to  $V_{\text{IP}}$ . If  $t_A$  cannot be observed as in Fig. 5C,  $t_{\text{res}}$  can be obtained by solving simultaneous functions expressing the progression of the boundaries A/AB and AB/B. In the present study  $t_{\text{res}}$  was obtained by this method. The boundary functions and the observed  $t_{\text{res}}$  for the SPADNS and MCA system are shown in Table II. The distance between the injection port and the first detector was *ca.* 16 cm

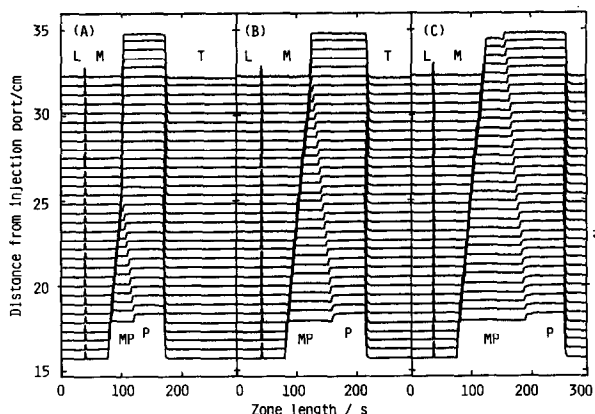


Fig. 6. Transient isotachopherogram of monochloroacetic acid and picric acid observed by the use of the 32-channel UV-photometric detector. The sample concentration was 5 mM and the amounts were (A) 15, (B) 20 and (C) 25 nmol. The leading electrolyte was 5 mM hydrochloric acid and the pH was adjusted to 3.6 (buffer  $\beta$ -alanine). The terminating electrolyte was 10 mM caproic acid. The migration current was 49.2  $\mu\text{A}$ . The I.D. of the separation tube was 0.51 mm.

in this case, however the observed values were not consistent as shown. This shows that the initial sample zone moved slightly when it was connected with the leading electrolyte by the valve V1 in Fig. 1. The probable error of  $t_{res}$  was within 20–30 s.

Fig. 6 shows the observed transient isotachopherogram of MCA and PIC on varying the sample amounts. The number of data used for the evolution was 1200 per channel. Small amounts of SPADNS were added to the mixture to distinguish the

TABLE III

DETECTOR POSITION, BOUNDARY-DETECTED TIME AND TIME-BASED ZONE LENGTH FOR THE MONOCHLOROACETIC ACID AND PICRIC ACID (1:1) SYSTEM

Operational system: leading electrolyte, 5mM hydrochloric acid- $\beta$ -alanine (pH 3.60). Current: 49.2  $\mu$ A. Diameter of the separation tube: 0.51 mm. Sample concentration: 4.6 mM. Sample amounts: each 15 nmol. —, Does not exist; ?, the exact boundary positions could not be estimated.

Detector position		Boundary-detected time (s)					Overall zone length (s)
No.	mm	L/M	M/MP	M/P	MP/P	P/T	
1	0	505.5	543.6	—	586.1	636.9	131.4
2	5.4	522.3	561.9	—	601.7	653.8	131.4
3	10.5	539.0	580.3	—	617.1	670.6	131.6
4	15.9	556.6	599.3	—	633.5	688.2	131.6
5	21.2	573.9	617.6	—	648.6	705.5	131.6
6	26.5	591.2	636.9	—	665.2	722.6	131.4
7	31.8	608.1	655.2	—	680.6	739.5	131.4
8	37.1	625.4	674.8	—	696.7	757.1	131.6
9	42.4	642.8	692.6	—	712.1	773.7	130.9
10	47.4	659.1	710.7	—	727.0	790.0	130.9
11	53.0	677.0	729.7	—	743.1	807.6	130.7
12	58.5	695.0	748.8	—	759.0	825.7	130.7
13	63.9	712.1	767.1	—	774.7	842.5	130.4
14	69.1	728.7	786.1	—	790.5	859.9	131.1
15	74.6	746.3	?	?	?	877.7	131.4
16	79.9	763.4	(59.3)*	822.8	(71.8)**	894.6	131.1
17	85.3	781.0	(59.6)	840.6	(71.6)	912.1	131.1
18	90.8	798.1	(59.8)	857.9	(71.8)	929.7	131.6
19	96.1	815.7	(59.8)	875.5	(72.5)	948.0	132.4
20	101.4	833.0	(60.1)	893.1	(71.8)	964.9	131.9
21	106.9	850.1	(60.6)	910.7	(72.5)	983.2	133.1
22	112.3	867.2	(60.8)	928.0	(72.8)	1000.8	133.6
23	117.8	885.0	(60.8)	945.8	(72.5)	1018.4	133.3
24	123.1	902.4	(61.1)	963.4	(72.0)	1035.5	133.1
25	128.4	919.5	(61.5)	981.0	(72.3)	1053.3	133.8
26	133.6	936.1	(61.8)	997.9	(72.3)	1070.2	134.1
27	138.9	953.4	(61.8)	1015.2	(72.5)	1087.7	134.3
28	144.2	970.8	(62.0)	1032.8	(72.0)	1104.8	134.1
29	149.6	988.3	(61.5)	1049.9	(72.3)	1122.2	133.8
30	154.8	1005.2	(62.0)	1067.2	(71.8)	1139.0	133.8
31	160.2	1023.3	(61.5)	1084.8	(71.6)	1156.4	133.1
32	165.5	1039.9	(62.3)	1102.1	(71.3)	1173.5	133.6

\* Zone length (s) of MCA.

\*\* Zone length (s) of PIC.

TABLE IV

OBSERVED BOUNDARY FUNCTIONS FOR THE MONOCHLOROACETIC ACID AND PICRIC ACID (1:1) SYSTEM AND THE RESOLUTION TIME

For the operational system, see Table III. For the definition of symbols, see Table II.

	Sample amount (nmol)								
	40			50			60		
	V	D	D <sub>0</sub>	V	D	D <sub>0</sub>	V	D	D <sub>0</sub>
L/M	3.099	-156.7	0	3.101	-157.0	0	3.104	-162.6	0
M/MP	2.847	-154.8	1.9	2.859	-156.0	1.0	2.857	-160.7	1.9
M/P	3.063	-172.1	-15.4	3.051	-176.8	-19.8	-	-	-
MP/P	3.380	-198.2	-41.5	3.368	-210.4	-53.4	3.333	-225.9	-65.2
P/T	3.081	-196.0	-39.3	3.079	-209.0	-52.0	3.076	-168.8	-66.9
<i>t</i> <sub>res</sub>	814			1069			1370		

leading zone. The sample concentration was 5 mM and the pH of the solution was 3.03. The sample amounts were (A) 15, (B) 20 and (C) 25 nmol. Table III shows the boundary-detected time in the separation process of the 15-nmol mixture. The boundary functions and the observed *t*<sub>res</sub> for the MCA and PIC system are shown in Table IV. The resolution time needed for the MCA/PIC system is twice as large as that of the SPADNS/MCA system. This is because the mobility difference between MCA and PIC is smaller than that between SPADNS and MCA. The effective mobilities  $\bar{m}$ , at the steady state were  $48 \cdot 10^{-5}$ ,  $35 \cdot 10^{-5}$  and  $29 \cdot 10^{-5}$  cm<sup>2</sup> V<sup>-1</sup> s<sup>-1</sup>.

Thus the present apparatus is very useful for the study of the transient state, although the samples are restricted. Namely, in the two-component system, at least one of the samples must be UV-absorptive. A detailed discussion of factors affecting the boundary velocities and the resolution time will be reported in the following paper.

## ACKNOWLEDGEMENTS

T. H. thanks the Ministry of Education, Science, and Culture of Japan for support of the part of this work under a Grant-in-Aid for Scientific Research (No. 61540423). The authors thank Fujikura Densen Co. for supplying the quartz optical fibres. They are also grateful for the helpful suggestions made by the referee, Dr. F. M. Everaerts (Eindhoven University of Technology, The Netherlands).

## REFERENCES

- 1 F. M. Everaerts, J. L. Beckers and Th. P. E. M. Verheggen, *Isotachopheresis*, Elsevier, Amsterdam, 1976.
- 2 T. Hirokawa and Y. Kiso, *J. Chromatogr.*, 257 (1983) 197.
- 3 T. Hirokawa, M. Nishino, N. Aoki, Y. Kiso, Y. Sawamoto, T. Yagi and J.-I. Akiyama, *J. Chromatogr.*, 271 (1983) D1.
- 4 T. Hirokawa and Y. Kiso, *J. Chromatogr.*, 260 (1983) 225.
- 5 F. E. P. Mikkers, F. M. Everaerts and J. A. F. Peek, *J. Chromatogr.*, 168 (1979) 293.
- 6 F. E. P. Mikkers, F. M. Everaerts and J. A. F. Peek, *J. Chromatogr.*, 168 (1979) 317.
- 7 E. Schumacher, in F. M. Everaerts (Editor), *Analytical Isotachopheresis*, Elsevier, Amsterdam, 1981.
- 8 W. Thormann, D. Arn and E. Schumacher, *Electrophoresis*, 5 (1984) 323.
- 9 W. Thormann, D. Arn and E. Schumacher, *Electrophoresis*, 6 (1985) 10.
- 10 L. Arlinger, *J. Chromatogr.*, 91 (1974) 785.
- 11 M. Svoboda and J. Vacik, *J. Chromatogr.*, 119 (1975) 539.